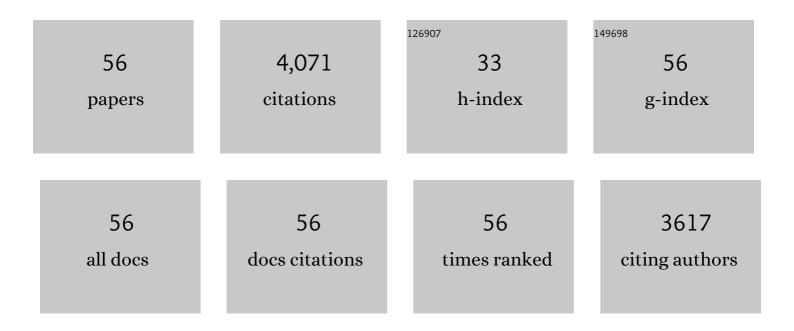
Fang Deng

List of Publications by Year in descending order

Source: https://exaly.com/author-pdf/9471083/publications.pdf Version: 2024-02-01



FANC DENC

#	Article	IF	CITATIONS
1	Identification and Regulation of Active Sites on Nanodiamonds: Establishing a Highly Efficient Catalytic System for Oxidation of Organic Contaminants. Advanced Functional Materials, 2018, 28, 1705295.	14.9	370
2	Potential Difference Driving Electron Transfer <i>via</i> Defective Carbon Nanotubes toward Selective Oxidation of Organic Micropollutants. Environmental Science & Technology, 2020, 54, 8464-8472.	10.0	288
3	Rapid toxicity elimination of organic pollutants by the photocatalysis of environment-friendly and magnetically recoverable step-scheme SnFe2O4/ZnFe2O4 nano-heterojunctions. Chemical Engineering Journal, 2020, 379, 122264.	12.7	238
4	Removal of Antimonite (Sb(III)) and Antimonate (Sb(V)) from Aqueous Solution Using Carbon Nanofibers That Are Decorated with Zirconium Oxide (ZrO ₂). Environmental Science & Technology, 2015, 49, 11115-11124.	10.0	233
5	Exceptional adsorption of arsenic by zirconium metal-organic frameworks: Engineering exploration and mechanism insight. Journal of Colloid and Interface Science, 2019, 539, 223-234.	9.4	213
6	The facile fabrication of novel visible-light-driven Z-scheme CuInS2/Bi2WO6 heterojunction with intimate interface contact by in situ hydrothermal growth strategy for extraordinary photocatalytic performance. Chemical Engineering Journal, 2019, 356, 819-829.	12.7	177
7	Gradient Hydrogen Migration Modulated with Self-Adapting S Vacancy in Copper-Doped ZnIn ₂ S ₄ Nanosheet for Photocatalytic Hydrogen Evolution. ACS Nano, 2021, 15, 15238-15248.	14.6	173
8	Revisiting the Graphitized Nanodiamond-Mediated Activation of Peroxymonosulfate: Singlet Oxygenation versus Electron Transfer. Environmental Science & Technology, 2021, 55, 16078-16087.	10.0	155
9	Lattice-Defect-Enhanced Adsorption of Arsenic on Zirconia Nanospheres: A Combined Experimental and Theoretical Study. ACS Applied Materials & Interfaces, 2019, 11, 29736-29745.	8.0	121
10	Design and synthesis of robust Z-scheme ZnS-SnS2 n-n heterojunctions for highly efficient degradation of pharmaceutical pollutants: Performance, valence/conduction band offset photocatalytic mechanisms and toxicity evaluation. Journal of Hazardous Materials, 2020, 392, 122345.	12.4	121
11	Visible-light-driven Z-scheme rGO/Bi ₂ S ₃ –BiOBr heterojunctions with tunable exposed BiOBr (102) facets for efficient synchronous photocatalytic degradation of 2-nitrophenol and Cr(<scp>vi</scp>) reduction. Environmental Science: Nano, 2019, 6, 3670-3683.	4.3	113
12	Evaluating the adsorptivity of organo-functionalized silica nanoparticles towards heavy metals: Quantitative comparison and mechanistic insight. Journal of Hazardous Materials, 2020, 387, 121676.	12.4	111
13	Efficient Removal of Antimony (III, V) from Contaminated Water by Amino Modification of a Zirconium Metal–Organic Framework with Mechanism Study. Journal of Chemical & Engineering Data, 2017, 62, 1519-1529.	1.9	93
14	MOF-derived magnetic porous carbon-based sorbent: Synthesis, characterization, and adsorption behavior of organic micropollutants. Advanced Powder Technology, 2017, 28, 1769-1779.	4.1	92
15	The band structure control of visible-light-driven rGO/ZnS-MoS2 for excellent photocatalytic degradation performance and long-term stability. Chemical Engineering Journal, 2018, 350, 248-256.	12.7	92
16	Heterogeneous Fenton-like catalysis of Fe-MOF derived magnetic carbon nanocomposites for degradation of 4-nitrophenol. RSC Advances, 2017, 7, 49024-49030.	3.6	87
17	Building electrode with three-dimensional macroporous interface from biocompatible polypyrrole and conductive graphene nanosheets to achieve highly efficient microbial electrocatalysis. Biosensors and Bioelectronics, 2019, 141, 111444.	10.1	81
18	Electrochemical recovery and high value-added reutilization of heavy metal ions from wastewater: Recent advances and future trends. Environment International, 2021, 152, 106512.	10.0	81

Fang Deng

#	Article	IF	CITATIONS
19	Enhanced photocatalytic degradation and H2 evolution performance of N CDs/S-C3N4 S-scheme heterojunction constructed by Ï€-ï€ conjugate self-assembly. Journal of Materials Science and Technology, 2022, 114, 222-232.	10.7	71
20	Recovery of Silver from Wastewater Using a New Magnetic Photocatalytic Ion-Imprinted Polymer. ACS Sustainable Chemistry and Engineering, 2017, 5, 2090-2097.	6.7	70
21	Porous Z-scheme MnO2/Mn-modified alkalinized g-C3N4 heterojunction with excellent Fenton-like photocatalytic activity for efficient degradation of pharmaceutical pollutants. Separation and Purification Technology, 2020, 246, 116890.	7.9	69
22	Solvothermal synthesis of Z-scheme AgIn5S8/Bi2WO6 nano-heterojunction with excellent performance for photocatalytic degradation and Cr(VI) reduction. Journal of Alloys and Compounds, 2019, 805, 41-49.	5.5	68
23	Removal of Cadmium(II) from Wastewater Using Novel Cadmium Ion-Imprinted Polymers. Journal of Chemical & Engineering Data, 2015, 60, 3253-3261.	1.9	66
24	Defect-rich porous carbon with anti-interference capability for adsorption of bisphenol A via long-range hydrophobic interaction synergized with short-range dispersion force. Journal of Hazardous Materials, 2021, 403, 123705.	12.4	66
25	Protonation of rhodanine polymers for enhancing the capture and recovery of Ag ⁺ from highly acidic wastewater. Environmental Science: Nano, 2019, 6, 3307-3315.	4.3	62
26	Thiol-rich, porous carbon for the efficient capture of silver: Understanding the relationship between the surface groups and transformation pathways of silver. Chemical Engineering Journal, 2022, 427, 131470.	12.7	60
27	A comparison of SMX degradation by persulfate activated with different nanocarbons: Kinetics, transformation pathways, and toxicity. Applied Catalysis B: Environmental, 2022, 310, 121345.	20.2	59
28	Activated biochar derived from pomelo peel as a high-capacity sorbent for removal of carbamazepine from aqueous solution. RSC Advances, 2017, 7, 54969-54979.	3.6	58
29	Double-defect-induced polarization enhanced OV-BiOBr/Cu2â^'xS high-low junction for boosted photoelectrochemical hydrogen evolution. Applied Catalysis B: Environmental, 2022, 314, 121502.	20.2	58
30	Nd ₂ (S, Se, Te) ₃ Colloidal Quantum Dots: Synthesis, Energy Level Alignment, Charge Transfer Dynamics, and Their Applications to Solar Cells. Advanced Functional Materials, 2016, 26, 254-266.	14.9	53
31	Rationally designed conjugated microporous polymers for contaminants adsorption. Science of the Total Environment, 2021, 750, 141683.	8.0	45
32	Efficient antimony removal by self-assembled core-shell nanocomposite of Co3O4@rGO and the analysis of its adsorption mechanism. Environmental Research, 2020, 187, 109657.	7.5	39
33	Synthesis of magnetic ion-imprinted fluorescent CdTe quantum dots by chemical etching and their visualization application for selective removal of Cd(II) from water. Colloids and Surfaces A: Physicochemical and Engineering Aspects, 2014, 462, 186-193.	4.7	36
34	High exposure effect of the adsorption site significantly enhanced the adsorption capacity and removal rate: A case of adsorption of hexavalent chromium by quaternary ammonium polymers (QAPs). Journal of Hazardous Materials, 2021, 416, 125829.	12.4	36
35	New insight on the adsorption capacity of metallogels for antimonite and antimonate removal: From experimental to theoretical study. Journal of Hazardous Materials, 2018, 346, 218-225.	12.4	35
36	Carbon quantum dot-sensitized and tunable luminescence of Ca ₁₉ Mg ₂ (PO ₄) ₁₄ :Ln ³⁺ (Ln ³⁺ =)	Tj <u>E</u> TQq0	0 0 rgBT /Ove

<i>via</i> a sol–gel process. Journal of Materials Chemistry C, 2019, 7, 2361-2375.

Fang Deng

#	Article	IF	CITATIONS
37	Simultaneous heavy metals removal via in situ construction of multivariate metal-organic gels in actual wastewater and the reutilization for Sb(V) capture. Chemical Engineering Journal, 2020, 400, 125359.	12.7	23
38	Reduced graphene oxide enhanced magnetic nanocomposites for removal of carbamazepine. Journal of Materials Science, 2018, 53, 15474-15486.	3.7	22
39	Insights into ion imprinted membrane with a delayed permeation mechanism for enhancing Cd2+ selective separation. Journal of Hazardous Materials, 2021, 416, 125772.	12.4	20
40	Electrodeposited graphene hybridized graphitic carbon nitride anchoring ultrafine palladium nanoparticles for remarkable methanol electrooxidation. International Journal of Hydrogen Energy, 2020, 45, 21483-21492.	7.1	19
41	Conducting polymer hydrogels as a sustainable platform for advanced energy, biomedical and environmental applications. Science of the Total Environment, 2021, 786, 147430.	8.0	19
42	Random Terpolymer Designed with Tunable Fluorescence Lifetime for Efficient Organic/Inorganic Hybrid Solar Cells. ACS Applied Materials & Interfaces, 2015, 7, 17408-17415.	8.0	17
43	Revisiting the adsorption of antimony on manganese dioxide: The overlooked dissolution of manganese. Chemical Engineering Journal, 2022, 429, 132468.	12.7	16
44	Facile solvothermal fabrication of cubic-like reduced graphene oxide/AgIn5S8 nanocomposites with anti-photocorrosion and high visible-light photocatalytic performance for highly-efficient treatment of nitrophenols and real pharmaceutical wastewater. Applied Catalysis A: General, 2018, 565, 170-180.	4.3	15
45	Monodisperse spherical sandwiched core-shell structured SiO2Au Ta2O5 and SiO2Au Ta3N5 composites as visible-light plasmonic photocatalysts. International Journal of Hydrogen Energy, 2018, 43, 20546-20562.	7.1	13
46	Engineering paths of sustainable and green photocatalytic degradation technology for pharmaceuticals and organic contaminants of emerging concern. Current Opinion in Green and Sustainable Chemistry, 2021, 29, 100465.	5.9	13
47	Bandgap engineering of hierarchical network-like SnIn4S8 microspheres through preparation temperature for excellent photocatalytic performance and high stability. Green Energy and Environment, 2019, 4, 264-269.	8.7	12
48	Tuning the performance of the non-fullerene organic solar cells by the polarizability. RSC Advances, 2018, 8, 3809-3815.	3.6	10
49	Insights into the binding manners of an Fe doped MOF-808 in high-performance adsorption: a case of antimony adsorption. Environmental Science: Nano, 2022, 9, 254-264.	4.3	10
50	Efficient heterojunction solar cells based on the synergy between planarity and dipole moment in fluorinated-thienothiophenes-based donor-acceptor polymers. Synthetic Metals, 2018, 245, 42-50.	3.9	9
51	Tandem type PRBs-like technology implanted with targeted functional materials for efficient resourceful treatment of heavy metal ions from mining wastewater. Chemical Engineering Journal, 2021, 420, 130506.	12.7	9
52	Synthesis of anatase TiO2 in a vinyl-containing ionic liquid and its enhanced photocatalytic activity. Research on Chemical Intermediates, 2013, 39, 2857-2865.	2.7	7
53	Bacteria-affinity aminated carbon nanotubes bridging reduced graphene oxide for highly efficient microbial electrocatalysis. Environmental Research, 2020, 191, 110212.	7.5	7
54	Perfluorinated conjugated microporous polymer for targeted capture of Ag(I) from contaminated water. Environmental Research, 2022, 211, 113007.	7.5	5

#	Article	IF	CITATIONS
55	Rapid and selective recycling of Ag(I) from wastewater through an allylrhodanine functionalized micro-filtration membrane. Chemical Engineering Journal, 2022, , 136376.	12.7	4
56	Tuning the fluorescence lifetime of donor polymers containing different proportion of electron withdrawing groups inhybrid solar cells. Synthetic Metals, 2016, 221, 19-24.	3.9	2